Journal of Applied Geophysics 150 (2018) 11–20

Contents lists available at ScienceDirect

Journal of Applied Geophysics

journal homepage: www.elsevier.com/locate/jappgeo

Estimating water volume stored in the south-eastern Greenland firn aquifer using magnetic-resonance soundings

Anatoly Legchenko [a,*], Clément Miège [b], Lora S. Koenig [c], Richard R. Forster [b], Olivia Miller [d], D.K. Solomon [d], Nicholas Schmerr [e], Lynn Montgomery [c,e], Stefan Ligtenberg [f], Ludovic Brucker [g,h]

[a] Univ. Grenoble Alps, Institute of Research for Development, IGE, France
[b] Department of Geography, University of Utah, USA
[c] University of Colorado, USA
[d] Department of Geology and Geophysics, University of Utah, USA
[e] Department of Geology, University of Maryland, USA
[f] Institute for Marine and Atmospheric Research Utrecht (IMAU), Utrecht University, The Netherlands
[g] NASA Goddard Space Flight Center, Cryospheric Sciences Laboratory, USA
[h] Universities Space Research Association, Goddard Earth Sciences Technology and Research Studies and Investigations, USA

ARTICLE INFO

Article history:
Received 30 September 2017
Received in revised form 8 January 2018
Accepted 9 January 2018
Available online 16 January 2018

Keywords:
Firn aquifer
Greenland ice sheet
MRS
SNMR
Water volume estimate

ABSTRACT

Recent observations of the Greenland ice sheet show an increase of the area affected by progressive melt of snow and ice, thus resulting in production of the additional meltwater. In 2011, an important storage of meltwater in the firn has been observed in the S-E Greenland. This water does not freeze during the wintertime and forms a perennial firn aquifer. The aquifer spatial extent has been initially monitored with combined ground and airborne radar observations, but these geophysical techniques are not able to inform us on the amount of meltwater stored at depth. In this study, we use the magnetic resonance soundings (MRS) method for estimating the volume of water stored in the Greenland ice sheet firn and mapping its spatial variability. Our study area covers a firn aquifer along a 16-km E-W transect, ranging between elevations of 1520 and 1760 m. In July 2015 and July 2016, we performed MRS measurements that allow estimating the water volume in the studied area as well as the one-year water volume evolution. Water storage is not homogeneous, fluctuating between 0.2 and 2 m^3/m^2, and contains discontinuities in the hydrodynamic properties. We estimate an average volume of water stored in the firn in 2016 to be 0.76 m^3/m^2, which corresponds to a 0.76-m-thick layer of bulk water. MRS monitoring reveals that from April 2015 to July 2016 the volume of water stored at the location of our transect increases by about 36%. We found MRS-estimated depth to water in a good agreement with that obtained with the ground penetrating radar (GPR).

1. Introduction

In recent decades, an accelerated loss of ice in the Greenland ice sheet observed since 1990s is explained by increasing surface snow and ice melt with consequent runoff (Harper et al., 2012; Fettweis et al., 2013; Enderlin et al., 2014; van den Broeke et al., 2016; Fettweis et al., 2017). Recently, extensive firn aquifers have been identified and mapped in the lower percolation zone of the southeast of the Greenland ice sheet at an elevation between 1300 and 1800 m with a typical depth to water between 10 and 30 m (Forster et al., 2014; Miège et al., 2016). Kuipers Munneke et al. (2014) explain this aquifer development by a combination of high melt and high accumulation of snow. Observations carried out in a similar percolation zone but in the west of Greenland by Machguth et al. (2016) suggest that the stored water may take part in interactions between meltwater and ice and may promote different mechanisms of water circulation, for example, early runoff. The aquifer water may also exit the system and contribute to hydrofracturing (Poinar et al., 2017) thus influencing englacial meltwater pathways and ice dynamics. The firn aquifer could also have an effect at more global scale. For example, Koenig et al. (2014) report a sea level rise estimate of 0.4 mm if the water stored in Greenland's firn aquifers would drain. Because of its importance, the firn aquifer has been intensively studied. The ground penetrating radar (GPR) surveys (Miège et al., 2013; Forster et al., 2014) and airborne radar (Miège et al., 2016) allow investigating the spatial-temporal extensions and evolution of the water table (top of the aquifer). Montgomery et al. (2017) report the used of seismic measurements for locating the thickness of the firn and estimating the water content in ice. Koenig et al. (2014) and Miller et al. (2017) use boreholes and ice samples for measuring the porosity and the hydraulic conductivity of the water-saturated firn, respectively. In the French Alps, at Tête Rousse glacier, Garambois

* Corresponding author.
E-mail address: anatoli.legtchenko@ird.fr (A. Legchenko).

https://doi.org/10.1016/j.jappgeo.2018.01.005
0926-9851/

et al. (2016) report a successful application of GPR and the magnetic resonance sounding (MRS) methods for investigating englacial water reservoir showing a 20% error in the MRS estimate of the water volume (Vincent et al., 2012; Legchenko et al., 2014). Reported results encouraged us to apply MRS for estimating the water volume in the Greenland firn aquifer in conjunction with an existing extensive GPR dataset. Before our study, application of MRS on the Greenland ice sheet was not reported in the literature, which required to carry out some adaptation of the measuring and interpretation procedures to field conditions. In this paper, we share out experience through presenting results of MRS application to investigation of this Greenland firn aquifer.

2. Background

Nuclear magnetic resonance (NMR) is a well-known phenomenon widely used in geophysics for investigating water and hydrocarbons in porous media (Slichter, 1990; Dunn et al., 2002). The MRS method, also known as the Surface NMR (SNMR), is a large-scale application of NMR to non-invasive groundwater investigations (Semenov et al., 1989). The MRS method is selectively sensitive to groundwater, which renders it an efficient tool for hydrogeology (Legchenko and Valla, 2002; Legchenko et al., 2002b; Legchenko, 2013; Behroozmand et al., 2015). Usually, NMR is applied in a small scale (samples or a local area around borehole) and calibration of the NMR signal is a relatively easy task. When using MRS however, the investigated area is large (many hundreds of cubic meters of the subsurface) and consequently, direct calibration of the MRS signal is challenging even when investigating a relatively homogeneous subsurface. For example, the use of rock samples for calibration may meet the scale-change problem (Müller-Petke et al., 2011b). Thus, the accuracy of the water volume estimate with MRS is largely dependent on the accuracy of the forward modeling and inversion.

The mathematical model for computing MRS signal has been developed in early 1980s and then progressively improved (Schirov et al., 1991; Weichman et al., 2000; Valla and Legchenko, 2002; Legchenko, 2004). The electrical conductivity of rocks has an effect on the magnetic resonance signal and it has to be taken into account in the mathematical model (Trushkin et al., 1995; Shushakov, 1996; Legchenko et al., 2008). Legchenko et al. (2010) adapted to MRS measuring conditions the spin-echo procedure necessary for measuring in the presence of magnetic rocks. It is an important issue because of neglecting the heterogeneity of the geomagnetic field may cause serious errors in interpretation (Vouillamoz et al., 2011). A simple and convincing verification of the MRS forward modeling consists of measuring MRS signal from the surface of frozen water reservoir, which allows an accurate verification of the water volume estimated with MRS (Schirov et al., 1991; Legchenko et al., 2004; Müller-Petke et al., 2011a). Recently reported results show that MRS is able to estimate the volume of water stored in a 3-D formation (Legchenko et al., 2011). Drainage of a subglacial cavern in the Tête Rousse glacier (French Alps) reveals a 20% error in the MRS estimate of the water volume (Vincent et al., 2012; Legchenko et al., 2014). Dlugosch et al. (2011) report a comparison of MRS results obtained with different MRS instruments at the same site. They have found a good correspondence in-between. All these experiments, as well as many others reported in the literature, confirm accuracy of the MRS mathematical model.

Inversion of MRS measurements gives access to the water content in the subsurface. The most popular method for resolving MRS inverse problem is the Tikhonov regularization (Legchenko and Shushakov, 1998; Mueller-Petke and Yaramanci, 2010.). However, other approaches like the block inversion (Mohnke and Yaramanci, 2002), laterally constrained inversion (Behroozmand et al., 2012) and Monte Carlo simulations (Guillen and Legchenko, 2002; Chevalier et al., 2014) also provide good results. Under specific conditions, inversion can be improved by optimizing the measuring procedure (Dalgaard et al., 2016; Pan et al., 2017). Hertrich (2008) and Behroozmand et al. (2015) provide the up to date reviews of MRS development. The MRS inverse problem is ill posed, which gives rise to the equivalence problem: different inverse models may generate similar signals. Thus, whatever will be inversion scheme the resolution of MRS inversion is limited (Müller-Petke and Yaramanci, 2008; Parsekian and Grombacher, 2015). Consequently, MRS users must consider this limitation for quantitative interpretation of MRS results.

3. Method

3.1. Forward modeling

For performing MRS measurements, we use a wire loop on the surface. The loop acts as a transmitter of an electromagnetic field and then, after the transmitting is terminated, as a receiver of the response from groundwater. Both the transmitting field and the receiving signal oscillate with the Larmor frequency ω_0, which is the resonance frequency for protons in the earth's magnetic field. One sounding consists of measuring the signal versus pulse moment $q = I_0\tau$, which is a product of the current amplitude I_0 and pulse duration τ. We assume the horizontal stratification of the subsurface and compute the amplitude of the magnetic resonance signal e_0 versus pulse moment as (Legchenko and Shushakov, 1998)

$$e_0(q) = \frac{\omega_0}{I_0}\int_z B_\perp M_\perp w(z)dz, \tag{1}$$

where $B_\perp$ is the component of the loop magnetic field transversal to the earth's magnetic field, $M_\perp$ is the transversal component of the nuclear magnetization and $w(z)$ is the water content distribution versus depth.

3.2. Inverse modeling

The water content in the subsurface $w(z)$ is a solution of the integral equation (Eq. (1)). For resolving this equation, we approximate it by a matrix equation

$$\mathbf{Aw} = \mathbf{e_0}, \tag{2}$$

where $\mathbf{A}$ is a rectangular matrix of $I \times J$, $\mathbf{e_0}$ is a set of experimental data of I and $\mathbf{w}$ is a water content vector of J. We define the depth z_j and the thickness Δz_j of layers in the inverse model that compose columns in the matrix $\mathbf{A}$ with respect to

$$\Delta z_j = z_{j+1} - z_j, \quad z_{\max} = \sum_{j=1}^{J}\Delta z_j, \tag{3}$$

where $\Delta z_1 \le \Delta z_2 \le .. \le \Delta z_j \le .. \le \Delta z_J$ and $z_{\max}$ is the maximum depth of investigation. Additionally, we impose the limitation $\Delta z_j \ge 0.5$ m. We apply the Tikhonov regularization method (Tikhonov and Arsenin, 1977), which provides an approximate solution of the Eq. (2) as a trade-off between the fitting error and the smoothness of the solution. For that, we minimize the Tikhonov functional $M(\alpha_T)$

$$M(\alpha_T) = \|\mathbf{Aw} - \mathbf{e_0}\|_{L_2} + \alpha_T\|\mathbf{w}\|_{L_2} = \min, \tag{4}$$

where $\alpha_T > 0$ is the smoothing factor. The Tikhonov solution with $\alpha_T = \tilde{\alpha}_T$ corresponds to $M(\tilde{\alpha}_T) = \min$ with the corresponding water content $\mathbf{w} = \mathbf{w}_T$.

MRS inversion provides the water content w_j for each horizontal infinite layer of the thickness Δz_j and consequently the volume of water per surface unit in a layer j is $V_j = w_j \times \Delta z_j$. Thus, the total volume of water per surface unit observed with one sounding is

$$V = \sum_{j=1}^{J}(V_j). \tag{5}$$

In general, solution of the Eq. (2) is non-unique and different equivalent inverse models ($\mathbf{w}_T$ is one of them) may provide different values of the water volume. For estimating uncertainty in the water volume estimate, Legchenko et al. (2017) report application of the Monte Carlo simulations around the inverse model obtained with the Tikhonov regularization. They propose to limit perturbations of the initial model within the uncertainty in the water content computed using the singular values decomposition (SVD). For estimating uncertainty, the minimum and the maximum volumes of water in the equivalent models are calculated. This approach allows to respect the smoothness constrain assumed for the inversion.

We also use the minimum and the maximum volumes of water for estimating the uncertainty, but in ice environment, the smoothness assumption is not always justified and for investigating the solution space around $\mathbf{w}_T$ we apply an arbitrary perturbation (Δw). In this study, we used $\Delta w = 0.05$. This value corresponds to about 30% of the maximum observed water content in Greenland. For sites with a small amount of water, it represents >100%. Thus, we obtain equivalent inverse models linked with the solution given by the Tikhonov regularization, but not necessary smooth at the end of the optimization. For generating an equivalent inverse model, we minimize two objective functions for the water content ($\mathbf{w}$) with fixed penalty weight ($\alpha_{\min}$ and $\alpha_{\max}$ for the minimum and the maximum volume solutions respectively).

$$\|\mathbf{Aw}-\mathbf{e_0}\|_{L_2} + \alpha_{\min} V(\mathbf{w}) = \min, \tag{6}$$

and

$$\|\mathbf{Aw}-\mathbf{e_0}\|_{L_2} + \frac{\alpha_{\max}}{V(\mathbf{w})} = \min, \tag{7}$$

where $V(\mathbf{w})$ is computed in accordance with Eq. (5). We use the conjugate gradients method for optimization and apply, as the first guess, $\mathbf{w}_T$ given by the Tikhonov regularization and an arbitrary constrain Δw

$$(w_{T,j} - \Delta w) \le w_j \le (w_{T,j} + \Delta w). \tag{8}$$

Resolution of the Eqs. (6) and (7) with different values of the penalty weight provides the misfits quantified computing the root mean square error ($RMSE(\alpha_{\min})$ and $RMSE(\alpha_{\max})$). We select $\alpha_{\min} = \tilde{\alpha}_{\min}$ and $\alpha_{\max} = \tilde{\alpha}_{\max}$ so that the misfit given by the corresponding solutions ($\mathbf{w} = \mathbf{w}_{\min}$ and $\mathbf{w} = \mathbf{w}_{\max}$) would be equal to the misfit of the solution given by the Tikhonov regularization

$$\begin{cases} RMSE(\tilde{\alpha}_{\min}, \mathbf{w}_{\min}) = RMSE(\tilde{\alpha}_T, \mathbf{w}_T) \\ RMSE(\tilde{\alpha}_{\max}, \mathbf{w}_{\max}) = RMSE(\tilde{\alpha}_T, \mathbf{w}_T) \end{cases} \tag{9}$$

Thus, these three equivalent inverse models provide an estimate of the water volume ($V_T(\mathbf{w}_T)$), with the uncertainty given by $V_{\min}(\mathbf{w}_{\min})$ and $V_{\max}(\mathbf{w}_{\max})$.

3.3. Estimated resolution

We estimate the resolution of the MRS inverse problem computing the minimum thickness of the model layers in the matrix **A** (Eq. (2)) that can be resolved by inversion under noiseless conditions (Legchenko and Pierrat, 2014). We discretize the subsurface and define the maximum number of the model layers so that the model resolution matrix computed with SVD is the identity matrix. We assume a 80-m-side square Tx/Rx loop and the maximum pulse moment of 3000 A-ms. With this setup, the maximum depth of detection of a 1-m-thick of bulk water, which we use for estimating the maximum depth of investigation, is approximately 80 m. Then, we obtained the minimum thickness of the model layers that can be resolved between 0 and 80 m as shown in Fig. 1.

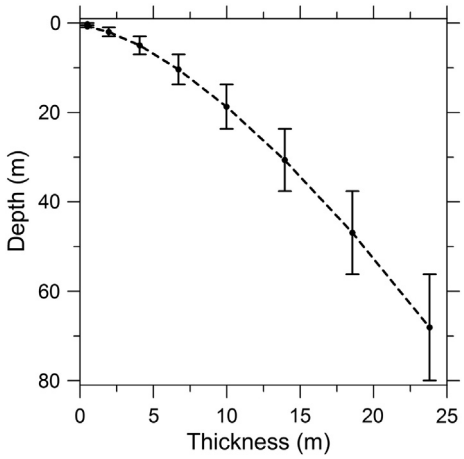

Fig. 1. The minimum thickness of the model layers that can be resolved versus layer depth computed considering the MRS field setup used during our study. The error bars show the top and the bottom of each model layer in the matrix **A**.

Fig. 1 shows that the resolution of the MRS inversion is progressively degrading with depth. Close to the surface a layer 0.5-m-thick can be resolved. However, only a much thicker layer (24 m) can be resolved at 68 m. For example, at the depth of 20 m a layer of about 10-m-thick can be resolved and we estimate the resolution at this depth as ±5 m. For investigating targets deeper than 30 m, we recommend a more powerful MRS instrument (NUMIS^{POLY} fabricated by IRIS Instruments (http://www.iris-instruments.com/) or GMR fabricated by VISTA CLARA Inc. (http://www.vista-clara.com/)) allowing better resolution.

3.4. Field setup

We use a square loop with the side length of 80 m and a NUMIS^{LITE} instrument (www.iris-instruments.com/) with the maximum amplitude of the current in the loop of about 80 A. With a 40-ms pulse, the maximum pulse moment is thus limited by approximately 3200 A-ms. These parameters of the measuring device allow the maximum depth of water detection in Greenland of approximately 80 m. The estimated resolution is shown in Fig. 1. All the MRS measurements, fulfilled during our study, are of a good quality (the noise level after stacking and filtering was varying between 8 and 10 nV with the signal amplitude ranging between 16 and 330 nV. One sounding requires between 2.5 and 3.5 h for measuring. Installation of 80 × 80 m^2 square loop by two persons takes about one hour. For data processing and inversion, we use SAMOVAR software package. For computing MRS signal using Eq. (1), we set the inclination of the Earth's magnetic field 75°N. The Larmor frequency, measured at each station with the proton magnetometer, is varying between 2296 and 2310 Hz. The resistivity of ice is set at 200 Ω-m and the water temperature at 0 °C. Boreholes and seismic study carried out in the area show no water below 36 m, which allows limiting MRS inversion by 36 m. We do not use other constrains.

3.5. Investigated area

The area investigated with MRS is located about 50 km West of Helheim glacier's terminus (Fig. 2). Airborne radar observations from NASA Operation IceBridge, GPR data, and boreholes provided the initial information about the aquifer characteristics. Based on airborne radar data and seismic measurements performed in 2015 and 2016, we find the ice thickness to be approximately 800 m (Montgomery et al., 2017). MRS surveys were carried in July–August of 2015 and 2016. The fieldwork was scheduled along a 16-km-long profile. It includes drilling boreholes, GPR, seismic and MRS surveys.

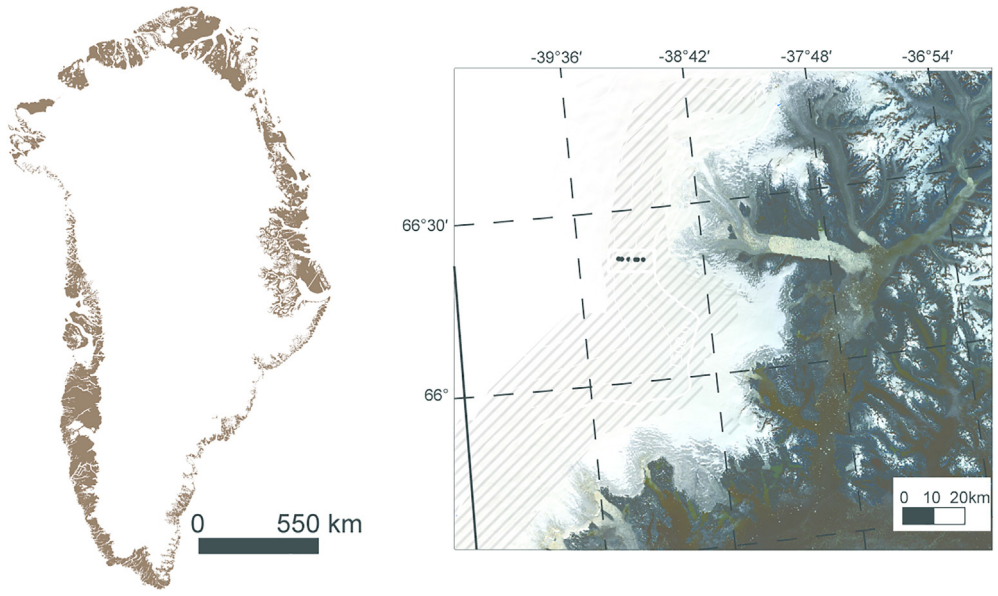

Fig. 2. Location map of the MRS survey in Greenland: a) position of the investigated area; b) study area upstream of Helheim glacier. Hatches represent the firn-aquifer presence derived from the airborne data (Miège et al., 2016). The background image is a Landsat image (USGS©) from August 6, 2017.

4. Results

4.1. Numerical modeling

For investigating accuracy of the water volume estimation with MRS, we use synthetic data computed assuming two models representing two time-lapse MRS soundings and considering the scenario of increasing volume of water in ice between these two soundings. Parameters of the models are inspired by typical parameters of the firn aquifer observed during our study. The "model-1" is composed of a water-saturated formation located at a depth of between 22 and 30 m and characterized by the water content $w = 5\%$ and the relaxation time $T_2^* = 300$ ms. The "model-2" is composed of the layer located between 20 and 30 m ($w = 6\%$ and $T_2^* = 600$ ms). Synthetic signals computed for these two models were contaminated with a 10-nV normally distributed random noise, which corresponds to the typical noise amplitudes after stacking observed during our campaigns. Fig. 3a shows the "model-1" and three inverse models provided by inversion of the synthetic data: inversion with the regularization and two inverse models corresponding to the maximum and the minimum volumes of water. Fig. 3b shows the "model-2" and three inverse models corresponding to inversion of the data set computed for this model. Fig. 3c shows the relaxation times corresponding to both models and the relaxation times recovered by inversion.

Synthetic signals and inversion fits corresponding to the inversion presented in Fig. 3 are shown in Fig. 4. For both initial models ("model-1" and "model-2"), the inverse models corresponding to V_T, $V_{\min}$ and $V_{\max}$ solutions fit synthetic data with respect to Eq. (9). The misfit ($RMSE_{\text{mod1}} \approx 5$ nV and $RMSE_{\text{mod2}} \approx 3$ nV) show that the inversion is correct and the inverse models can be considered as equivalent.

Table 1 summarizes estimation of the volume of water per surface unit corresponding to this synthetic example. Our results show that for both models, the volume of water was estimated with the uncertainty better than ±20%. The difference in the water volume between the

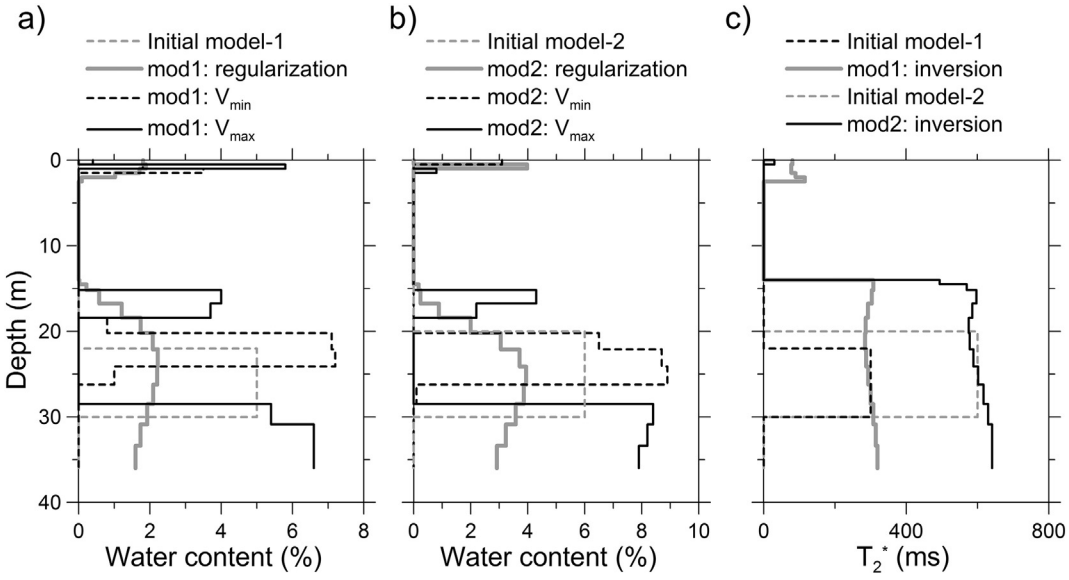

Fig. 3. Example of inversion of the synthetic data. MRS provided water content versus depth corresponding to the "model-1" (a) and to the "model-2" (b). The relaxation time T_2^* versus depth (c) corresponds to the solution with regularization for T_2^*.

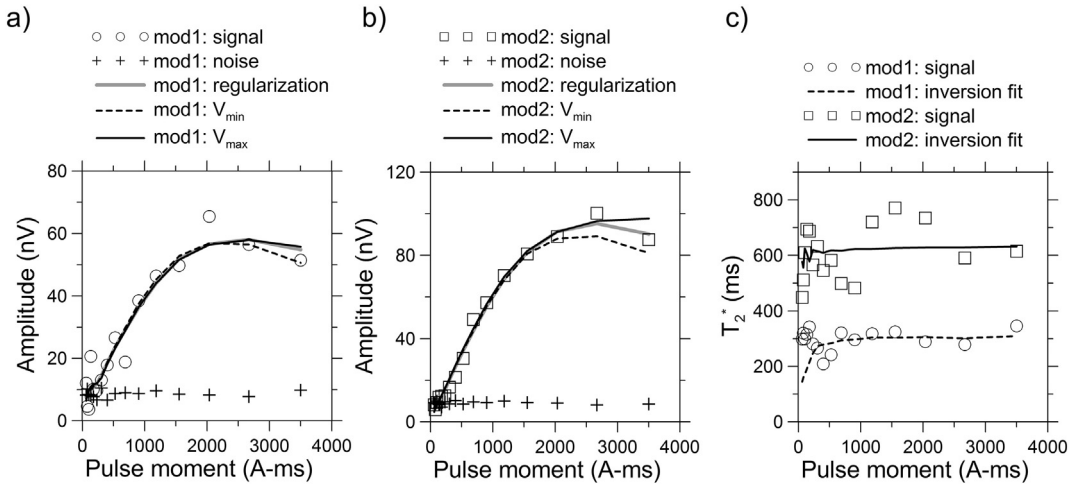

Fig. 4. MRS signals corresponding to the example of inversion of synthetic data presented in the previous figure. The amplitude (a, b) and relaxation time T_2^* (c) show synthetic data and the theoretical signals for each inverse model.

"model-1" and "model-2" is 0.2 m^3/m^2, which corresponds to 50% increase of the water volume. The modeling results suggest that the accuracy of the absolute MRS measurements of the water volume allows distinguishing between these two models. It is important to note that the ratio between the volumes given by the same type of the inverse models (V_T, V_{min} and V_{max}) is more stable than the estimation of the absolute volume of water. This propriety of MRS inversion suggests that the MRS monitoring of the water volume variations will be more accurate than estimation of the water volume with each individual sounding.

4.2. Field results

Accuracy of MRS monitoring is directly dependent of the accuracy and stability of the measuring device. During our study in Greenland, we used the same instrument and we verified it before and after deployment. For verification, we used the test site near Grenoble, France with known MRS response. At one site in Greenland, we made repetitive measurements using the same loop. In order to verify influence of the absence of the internal gradients of the magnetic field, we performed one sounding with a 40-ms-pulse and one with a 10-ms-pulse. Fig. 5 shows the amplitude of MRS signal provided by these two soundings versus pulse moment. One can see that the difference caused by the instrument instability is smaller than 5 nV. We also observe long values of the relaxation time T_2^*, which suggest small effect of the surface relaxation around ice particles.

Signal processing and inversion are done by applying to all MRS soundings the procedure described above. Boreholes and seismic measurements suggest that the bottom of the firn aquifer is not deeper than 32–34 m (Montgomery et al., 2017). It allows us to limit the maximum depth for inversion of MRS data at 36 m. Fig. 6 presents an example of MRS results obtained in 2016 at two stations. MRS8 station is located uphill of the profile and ice in this area contains very little amount of water. MRS3 station is located downhill and this sounding shows the maximum volume of water observed during our survey. MRS8 sounding shows 1 to 4% of water in the shallow depth, which can be attributed to seasonal meltwater in the firn (Fig. 6a). This sounding detects no aquifer. Inversion of MRS3 data (Fig. 6b) shows the main water reservoir located between 20 and 26 m with the water content of 15% approximately. Some smaller amount of water may be located below 26 m and the top of this aquifer is located between 18 and 21 m. Fig. 6c shows the relaxation times. The relaxation time is long for both soundings because of low surface relaxivity rate in the snow and firn. As expected, in the unsaturated zone (MRS8) the relaxation time is shorter in comparison with the aquifer (MRS3). For both soundings, the maximum-volume inverse models show water below 30 m. From the mathematical point of view, we cannot exclude this possibility. However, this deeper water is not confirmed by borehole and seismic measurements. MRS alone cannot resolve this layer due to the limited resolution at this depth (Fig. 1).

Measured data and inversion fits corresponding to these two stations are presented in Fig. 7.

Table 2 presents the volume of water estimated with MRS3 and MRS8 soundings. The uncertainty $\Delta V_{min} = 100\,\% \times (V_{min} - V_T)/V_T$ and $\Delta V_{max} = 100\,\% \times (V_{max} - V_T)/V_T$ shows the accuracy of the water volume estimate given by the solution with the regularization.

MRS3 sounding exhibits much larger amplitude of the MRS signal in comparison with MRS8 because of 15 folds larger volume of water in the firn. Consequently, the signal to noise ratio is also better for this station. It yields to smaller uncertainty in estimation of the water volume. Both stations provide better estimation of the minimum volume than the maximum one, which can be explained by a poor resolution of MRS inversion for deep layers, which may bias the water volume estimate.

We performed time-lapse MRS measurements at the same place in Greenland, which allows a one-year monitoring of the water volume stored in the ice sheet firn. An example of such type of measurements is presented in Fig. 8. Fig. 8a shows the water content versus depth. The observed difference between 2015 and 2016 suggests that the maximum water content in firn was not changing, but the thickness of the aquifer increased. Fig. 8b shows the amplitude of the MRS signal versus pulse moment. The theoretical signals computed after inversion results fit well experimental data. The increase of the observed amplitude in the late July of 2016 relative one measured in late July 2015 is above the noise level and we attribute it to the additional water stored in the firn.

Table 3 presents the volume of water computed after inversion results. Considering the inverse solution with the Tikhonov regularization, we can estimate the increase of the volume of water as: $100\% \times (1.71 - 1.14) / 1.14 = 50\%$.

Table 1
Summary of water volume estimates for two synthetic data sets corresponding to the "model-1" and "model-2".

Model	V_{true} (m^3/m^2)	V_{min} (m^3/m^2)	V_T (m^3/m^2)	V_{max} (m^3/m^2)	ΔV_{max} (%)	ΔV_{min} (%)
model-1	0.40	0.34	0.4	0.47	17.5	−15.0
model-2	0.60	0.50	0.62	0.72	20.0	−16.7
Difference (V_{mod2}-V_{mod1})	0.2	0.16	0.22	0.25		
Ratio (V_{mod2}/V_{mod1})	1.50	1.47	1.55	1.53		

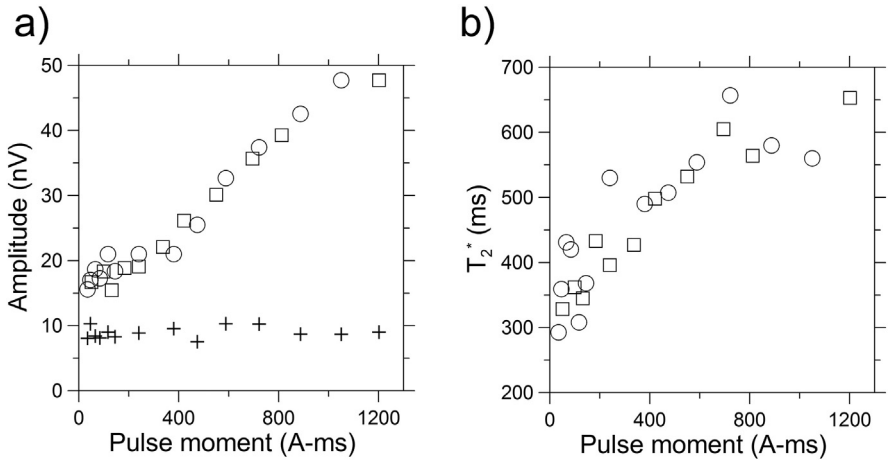

Fig. 5. Example of MRS measurements: a) amplitude of the MRS signal versus pulse moment for two soundings performed at the same site using a 40-ms-pulse (circles) and a 10-ms-pulse (squares); b) corresponding relaxation time T_2^* versus pulse moment. Crosses show the noise level after stacking.

Fig. 9 presents a summary of MRS results corresponding to all sites investigated in 2015 and 2016. Position of MRS stations along profile with their altitudes (Fig. 9a) provides extension of the aquifer from inland, higher elevations to lower elevations. Both airborne and ground radars do not show reflections that may correspond to the aquifer higher than MRS8 station, which also shows no water

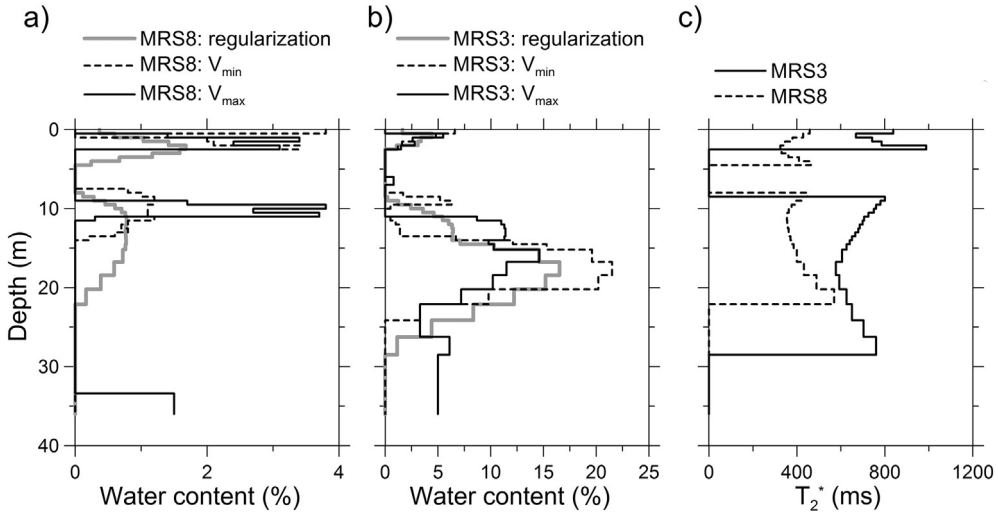

Fig. 6. MRS provided water content versus depth corresponding to the MRS8 station (a) located in the area with little water and the MRS3 station (b) located in the area with an important amount of water accumulation in ice. The MRS water content corresponds to the inverse models obtained with the regularization (gray line) and the inverse models with the minimum and maximum volumes of water (dashed and solid lines respectively). The relaxation time T_2^* (c) versus depth corresponds to the regularization solution for these two stations.

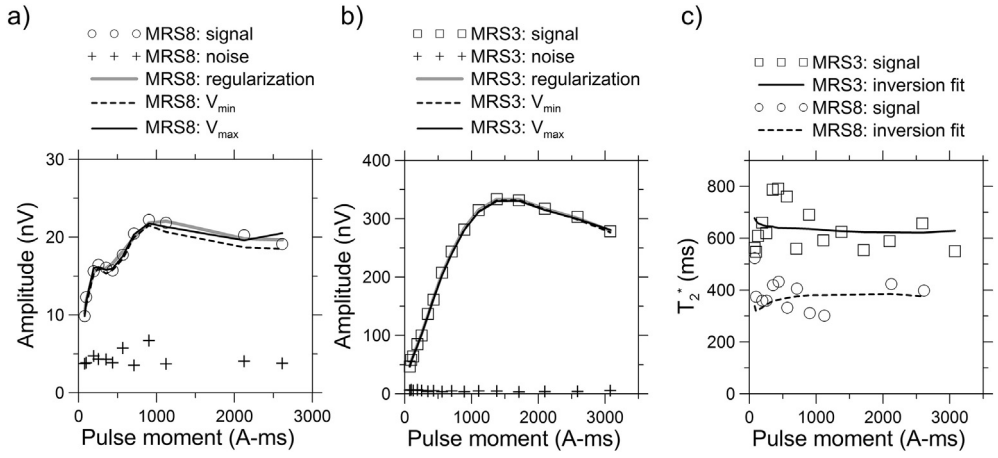

Fig. 7. Measured amplitude (a, b) and relaxation time T_2^* (c) corresponding to the inversion example presented in the previous figure. Lines show the theoretical signal for each inverse model.

Table 2
Summary of water volume estimates for two stations: MRS3 and MRS8.

Station	V_{min} (m^3/m^2)	V_T (m^3/m^2)	V_{max} (m^3/m^2)	ΔV_{max} (%)	ΔV_{min} (%)
MRS3	1.65	1.71	1.91	11.7	−3.5
MRS8	0.11	0.12	0.18	50.0	−8.3

Table 3
Summary of water volume estimates for the station MRS3 carried out in 2015 and 2016.

Station	V_{min} (m^3/m^2)	V_T (m^3/m^2)	V_{max} (m^3/m^2)	ΔV_{max} (%)	ΔV_{min} (%)
MRS3-2015	1.11	1.14	1.3	14.0	−2.6
MRS3-2016	1.65	1.71	1.91	11,7	−3,5

(Fig. 9b). Projection of the MRS water content logs onto GPR profile also fulfilled in 2016 Fig. 9b allows direct comparison in-between.

In general, we find MRS and GPR results consistent in-between. For example, MRS7 and MRS8 stations show a low water content and the GPR profile, at these locations, shows an absence of internal reflectors from the top of the aquifer observed at other stations. An area with smaller amount of stored water (MRS7) may correspond to a hydraulic barrier between the uphill and downhill areas. Scattered water storage in the downhill area located between 13 and 16 km suggests that the firn-and-ice formation may be heterogeneous in the shallow part (0–35 m). Fig. 9c presents the volume of water plotted against the distance along profile for all MRS soundings. The volume is computed after inverse models obtained with the regularization (V_T inverse model). The error bars show the volume of water computed after V_{min} and V_{max} inverse models corresponding to the minimum and the maximum volumes of water. Limited number of MRS soundings performed in 2015 does not allow estimation of the water volume variations between 2015 and 2016 in the uphill area located between 0 and 13 km (Fig. 9). In the downhill area however, MRS clearly shows larger amount of water observed at the same location in 2016. The increase of the volume is not homogeneous as could be expected and we explain it by redistribution of water in firn due to englacial water flows that may take place in this rather heterogeneous formation close to the crevasses area.

Table 4 presents a summary of the water volume estimation provided by MRS.

5. Discussion

For this survey, we applied the MRS method, which provides quantitative estimation of the volume of water in the aquifer unavailable with other surface geophysical methods. During this study, we have found an overall agreement between MRS, GPR, boreholes and seismic measurements (detection and localization of the aquifer formation). Before our survey, MRS has not been used in the Greenland ice sheet and there was no reference point to inform us regarding the measuring conditions to expect. Therefore, we transferred our knowledge gained from alpine glaciers, where MRS results have been verified by boreholes and pumping (Legchenko et al., 2011; Vincent et al., 2012; Legchenko et al., 2014). Additionally, we paid attention to verification of the measuring device, which is particularly important for time-lapse measurements. Thus, we consider that MRS provides reliable quantitative information about the volume of water in the firn. Numerical modeling results suggest an overall uncertainty of the water volume estimate with the MRS to be approximately ±20%.

Using time-lapse MRS measurements performed in 2015 and 2016 we estimate a one-year evolution of the water volume stored in the firn. Fig. 9c shows the water volume in the lower part of the profile (between 8 and 16 km). We compute the volume of water estimated with MRS stored in a band of one-m-wide and approximately 8 km long. We use the volume per square meter derived from MRS results and apply the linear interpolation between MRS stations. We find the volume estimated in 2015 as 4216 m^3 and in 2016 as 5719 m^3. Thus, a one-year increase of the volume of water stored in the firn along the investigated profile in 2016 is 1503 m^3, which corresponds to a 36% increase relative the volume observed in 2015.

For estimating the volume of water stored in the firn aquifer, we compute the volume of water estimated with MRS along the investigated profile in 2016 (Fig. 9c) stored in one-m-wide band and 15.77 km long. Results yield 12,035.5 m^3 per one-meter band. We obtain an average volume of water per square meter of the profile as $12{,}035.5/15770 = 0.76\ m^3/m^2$, which corresponds to a 0.76-m-thick layer of bulk water (with $w = 1$). A limited number of soundings fulfilled in 2015 does not allow us to make similar estimation for 2015.

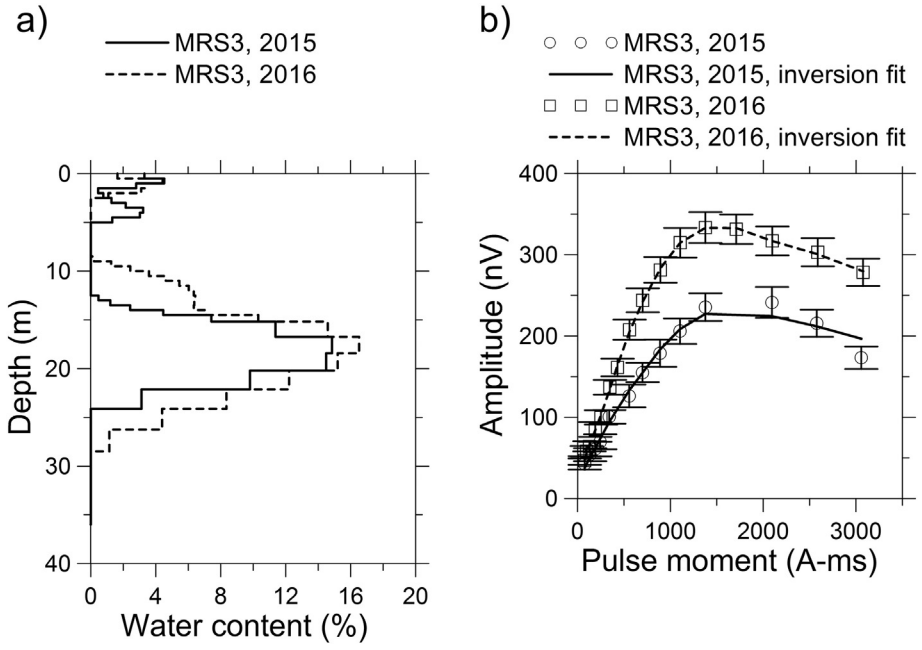

Fig. 8. MRS provided water content versus depth (a) and corresponding amplitudes of the MRS signal (b) obtained at the same site in 2015 and 2016. The error bars show uncertainty in measured data.

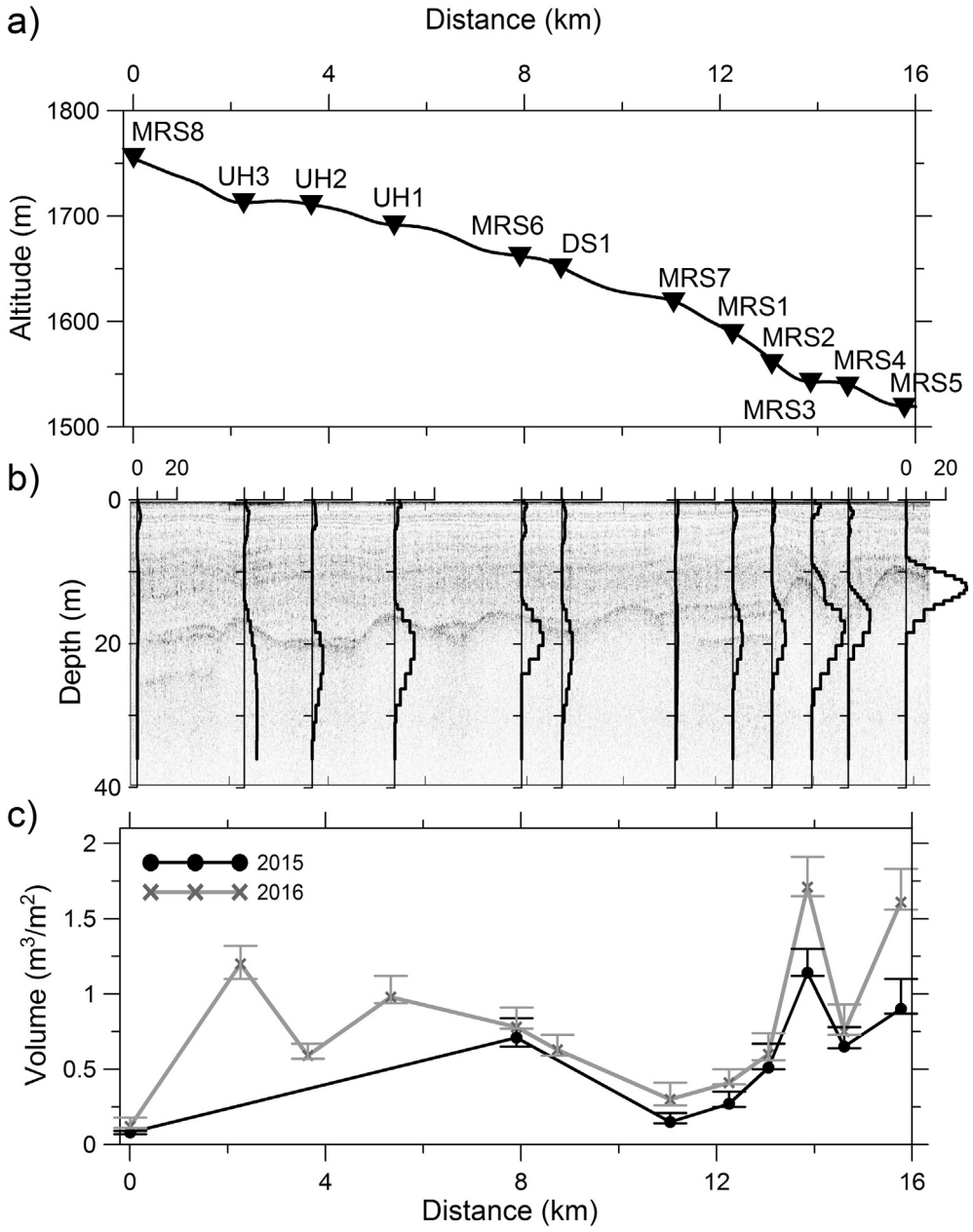

Fig. 9. Summary of MRS and GPR results. a) location of 2016 MRS stations along the profile investigated in Greenland; b) corresponding MRS water content (%) plotted in the same horizontal scale (0–20%) for all the stations projected onto the GPR profile both recorded in 2016; c) volume of water per surface unit computed after MRS results of 2015 (black line) and 2016 (gray line) plotted against position of MRS stations along profile. The error bars show the water volume provided the V_{min} and V_{max} inverse models.

Table 4
Summary of the water volume estimates after MRS results in Greenland. The volume of water corresponding to the V_T inverse model ranges between the estimates provided by V_{min} and V_{max} solutions.

Station	Latitude	Longitude	Distance (km)	Altitude (m)	Volume-2015 (m^3/m^2)	Volume-2016 (m^3/m^2)
MRS8	66.3673	−39.4839	0.00	1754.85	0.07 ≤ 0.08 ≤ 0.09	0.11 ≤ 0.12 ≤ 0.18
UH3	66.3657	−39.4337	2.26	1711.74	n/a	1.1 ≤ 1.20 ≤ 1.32
UH2	66.3650	−39.4029	3.64	1710.04	n/a	0.57 ≤ 0.59 ≤ 0.67
UH1	66.3639	−39.3651	5.33	1690.88	n/a	0.94 ≤ 0.98 ≤ 1.12
MRS6	66.3617	−39.3079	7.91	1661.10	0.65 ≤ 0.71 ≤ 0.84	0.77 ≤ 0.78 ≤ 0.91
DS1	66.3608	−39.2892	8.75	1649.99	n/a	0.59 ≤ 0.63 ≤ 0.73
MRS7	66.3579	−39.2382	11.05	1617.83	0.14 ≤ 0.15 ≤ 0.21	0.26 ≤ 0.3 ≤ 0.41
MRS1	66.3564	−39.2117	12.25	1587.88	0.25 ≤ 0.27 ≤ 0.35	0.4 ≤ 0.41 ≤ 0.5
MRS2	66.3554	−39.1938	13.06	1559.34	0.5 ≤ 0.51 ≤ 0.67	0.56 ≤ 0.60 ≤ 0.74
MRS3	66.3545	−39.1761	13.86	1541.62	1.11 ≤ 1.14 ≤ 1.3	1.65 ≤ 1.71 ≤ 1.91
MRS4	66.3538	−39.1593	14.61	1537.87	0.64 ≤ 0.65 ≤ 0.78	0.73 ≤ 0.75 ≤ 0.93
MRS5	66.3531	−39.1334	15.77	1517.95	0.85 ≤ 0.9 ≤ 1.1	1.56 ≤ 1.61 ≤ 1.83

Miège et al. (2016) estimate the surface area of the entire firn aquifer as 17,920 km^2. Assuming the regular structure of the aquifer similar to out transect studied with MRS, we may estimate the total volume of water stored in the firn aquifer in July 2016 as $0.76 \times 17{,}920 \times 10^6 = 1.37 \times 10^{10}$ m^3. For illustrating how much water represents this volume, let us compare it with the average annual discharge of the Amazon River estimated by Gupta (2007) as 209 m^3/s. We compute the average annual volume of water transported by the Amazon River to the sea (6.6×10^9 m^3). The ratio between the volume of water possibly stored in the firn aquifer and the average annual discharge of the Amazon River is $1.37 \times 10^{10}/6.6 \times 10^9 = 2.07$. This simple estimate shows that in July 2016 the firn aquifer contained the volume of water corresponding to about two-year discharge of the Amazon River. However, the impact of this stored water on the sea level rise (local or global) largely depends on the englacial water pathways and discharge mechanisms, which remain beyond the scope of this study.

Based on insufficient coverage of the entire aquifer area with geophysical and other measurements, extrapolation of our result to other areas in Greenland is an approximation. Despite of that, we hope that they may provide a first-order volume estimate that can contribute to validation of numerical models and more accurate mass balance estimates.

6. Conclusions

Our experience demonstrated that MRS appears to be an efficient tool suitable for using under Greenland ice sheet conditions. We found our results obtained with the MRS to be consistent with other available information about water storage in the firn. Additionally, MRS provides an estimate of the volume of water stored in ice, which is more difficult to obtain with other geophysical methods.

Our two-year study along a 16-km-long profile confirms that the firn aquifer is located between 20 and 30 m deep. We estimate the total volume of water stored in this area in 2016 as 0.76 m^3/m^2, which corresponds to a 0.76-m-thick layer of bulk water. Our results obtained in the restricted area demonstrate the possibility of estimating the volume of water stored in the entire aquifer. For that, an appropriate coverage of the aquifer area will be necessary. The time-lapse MRS measurements carried out in July 2015 and July 2016 show 36% increase of the volume of water stored in the area investigated with MRS.

Acknowledgements

Our work was supported by a grant (Investissements d'avenir – ANR10 LABX56) from Labex OSUG@2020. The authors acknowledge the French National Program (ANR)" Investment for Future - Excellency Equipment" project EQUIPEX CRITEX (grant # ANR-11-EQPX-0011) provided MRS equipment for the fieldwork. The field study in Greenland was made possible due to financial support provided by the U.S. National Science Foundation (Proposal Number: NSF-PLR-1417987 and NSF-PLR-1417993). We acknowledge CH2MHILL Polar Services for organizing the field logistics and thank them for an outstanding support during the 2015 and 2016 expeditions.

References

Behroozmand, A., Auken, E., Fiandaca, G., Christiansen, A.V., 2012. Improvement in MRS parameter estimation by joint and laterally constrained inversion of MRS and TEM data. Geophysics 77:WB191–WB200. https://doi.org/10.1190/GEO2011-0404.1.

Behroozmand, A.A., Keating, K., Auken, E., 2015. A review of the principles and applications of the NMR technique for near-surface characterization. Surv. Geophys. 36 (1):27–85. https://doi.org/10.1007/s10712-014-9304-0.

van den Broeke, M.R., Enderlin, E.M., Howat, I.M., Kuipers Munneke, P., Noël, B.P.Y., van de Berg, W.J., van Meijgaard, E., Wouters, B., 2016. On the recent contribution of the Greenland ice sheet to sea level change. Cryosphere 10:1933–1946. https://doi.org/10.5194/tc-10-1933-2016 (2016).

Chevalier, A., Legchenko, A., Girard, J.F., Descloitres, M., 2014. 3D Monte Carlo inversion of magnetic resonance measurements. Geophys. J. Int. 198 (1):216–228. https://doi.org/10.1093/gji/ggu091.

Dalgaard, E.M., Müller-Petke, M., Auken, E., 2016. Enhancing SNMR model resolution by selecting an optimum combination of pulse moments, stacking, and gating. Near Surf. Geophys. 14 (3):243–253. https://doi.org/10.3997/1873-0604.2016004.

Dlugosch, R., Mueller-Petke, M., Guenther, T., Costabel, S., Yaramanci, U., 2011. Assessment of the potential of a new generation of surface NMR instruments. Near Surf. Geophys. 9:89–102. https://doi.org/10.3997/1873-0604.2010063.

Dunn, K.J., Bergman, D.J., Latorraca, G.A., 2002. Nuclear Magnetic Resonance Petrophysical and Logging Applications. Elsevier Science Ltd, UK.

Enderlin, E.M., Howat, I.M., Jeong, S., Noh, M.-J., van Angelen, J.H., van den Broeke, M.R., 2014. An improved mass budget for the Greenland ice sheet. Geophys. Res. Lett. 41: 866–872. https://doi.org/10.1002/2013GL059010.

Fettweis, X., Franco, B., Tedesco, M., van Angelen, J.H., Lenaerts, J.T.M., van den Broeke, M.R., Gallée, H., 2013. Estimating the Greenland ice sheet surface mass balance contribution to future sea level rise using the regional atmospheric climate model MAR. Cryosphere 7 (2):469–489. https://doi.org/10.5194/tc-7-469-2013.

Fettweis, X., Box, J.E., Agosta, C., Amory, C., Kittel, C., Lang, C., van As, D., Machguth, H., Gallée, H., 2017. Reconstructions of the 1900–2015 Greenland ice sheet surface mass balance using the regional climate MAR model. Cryosphere 11:1015–1033. https://doi.org/10.5194/tc-11-1015-2017.

Forster, R.R., Box, J.E., van den Broeke, M.R., Miège, C., Burgess, E.W., van Angelen, J.H., Lenaerts, J.T.M., Koenig, L.S., Paden, J., Lewis, C., Gogineni, S.P., Leuschen, C., McConnell, J.R., 2014. Extensive liquid meltwater storage in firn within the Greenland ice sheet. Nat. Geosci. 7:95–98. https://doi.org/10.1038/ngeo2043.

Garambois, S., Legchenko, A., Vincent, C., Thibert, E., 2016. Ground-penetrating radar and surface nuclear magnetic resonance monitoring of an englacial water-filled cavity in the polythermal glacier of Tête Rousse. Geophysics 81 (1):WA131–WA146. https://doi.org/10.1190/GEO2015-0125.1.

Guillen, A., Legchenko, A., 2002. Inversion of surface nuclear magnetic resonance data by an adapted Monte Carlo method applied to water resource characterization. J. Appl. Geophys. 50:193–205. https://doi.org/10.1016/S0926-9851(02)00139-8.

Gupta, A., 2007. Large Rivers: Geomorphology and Management. John Wiley and Sons 978-0-470-84987-3.

Harper, J., Humphrey, N., Pfeffer, W.T., Brown, J., Fettweis, X., 2012. Greenland ice sheet contribution to sea-level rise buffered by meltwater storage in firn. Nature 491 (7423):240–243. https://doi.org/10.1038/nature11566.

Hertrich, M., 2008. Imaging of groundwater with nuclear magnetic resonance. Prog. Nucl. Magn. Reson. Spectrosc. 53 (4):227–248. https://doi.org/10.1016/j.pnmrs.2008.01.002.

Koenig, L.S., Miege, C., Forster, R.R., Brucker, L., 2014. Initial in situ measurements of perennial meltwater storage in the Greenland firn aquifer. Geophys. Res. Lett. 41 (1):81–85. https://doi.org/10.1002/2013GL058083.

Kuipers Munneke, P., Ligtenberg, S.R.M., van den Broeke, M.R., van Angelen, J.H., Forster, R.R., 2014. Explaining the presence of perennial liquid water bodies in the firn of the Greenland ice sheet. Geophys. Res. Lett. 41:476–483. https://doi.org/10.1002/2013GL058389.

Legchenko, A., 2013. Magnetic resonance imaging for groundwater. Wiley-ISTE 978-1-84821-568-9.

Legchenko, A., Pierrat, G., 2014. Glimpse into the design of MRS instrument. Near Surf. Geophys. 12:297–308. https://doi.org/10.3997/1873-0604.2014006.

Legchenko, A.V., Shushakov, O.A., 1998. Inversion of surface NMR data. Geophysics 63: 75–84. https://doi.org/10.1190/1.1444329.

Legchenko, A., Valla, P., 2002. A review of the basic principles for proton magnetic resonance sounding measurements. J. Appl. Geophys. 50:3–19. https://doi.org/10.1016/S0926-9851(02)00127-1.

Legchenko, A., Baltassat, J.-M., Beauce, A., Bernard, J., 2002. Nuclear magnetic resonance as a geophysical tool for hydrogeologists. J. Appl. Geophys. 50:21–46. https://doi.org/10.1016/S0926-9851(02)00128-3.

Legchenko, A., 2004. Magnetic Resonance Sounding: Enhanced Modeling of a Phase Shift. Applied Magnetic Resonance 25:621–636. https://doi.org/10.1007/BF03166553.

Legchenko, A., Baltassat, J.-M., Bobachev, A., Martin, C., Robin, H., Vouillamoz, J.-M., 2004. Magnetic resonance sounding applied to aquifer characterization. J. Groundwater 42 (3):363–373. https://doi.org/10.1111/j.1745-6584.2004.tb02684.x.

Legchenko, A., Ezersky, M., Girard, J.-F., Baltassat, J.-M., Boucher, M., Camerlynck, C., Al-Zoubi, A., 2008. Interpretation of magnetic resonance soundings in rocks with high electrical conductivity. J. Appl. Geophys. 66:118–127. https://doi.org/10.1016/j.jappgeo.2008.04.002.

Legchenko, A., Vouillamoz, J.M., Roy, J., 2010. Application of the magnetic resonance sounding method to the investigation of aquifers in the presence of magnetic materials. Geophysics 75 (6):L91–L100. https://doi.org/10.1190/1.3494596.

Legchenko, A., Descloitres, M., Vincent, C., Guyard, H., Garambois, S., Chalikakis, K., Ezersky, M., 2011. Three-dimensional magnetic resonance imaging for groundwater. New J. Phys. 13, 025022. https://doi.org/10.1088/1367-2630/13/2/025022.

Legchenko, A., Vincent, C., Baltassat, J.M., Girard, J.F., Thibert, E., Gagliardini, O., Descloitres, M., Gilbert, A., Garambois, S., Chevalier, A., Guyard, H., 2014. Monitoring water accumulation in a glacier using magnetic resonance imaging. Cryosphere 8 (155–166): 2014. https://doi.org/10.5194/tc-8-155-2014.

Legchenko, A., Comte, J.-C., Ofterdinger, U., Vouillamoz, J.-M., Lawson, F.M.A., Walsh, J., 2017. Joint use of singular value decomposition and Monte-Carlo simulation for estimating uncertainty in surface NMR inversion. J. Appl. Geophys. 144:28–36. https://doi.org/10.1016/j.jappgeo.2017.06.010.

Machguth, H., MacFerrin, M., van As, D., Box, J.E., Charalampidis, C., Colgan, W., Fausto, R.S., Meijer, H.A.J., Mosley-Thompson, E., van de Wal, R.S.W., 2016. Greenland meltwater storage in firn limited by near-surface ice formation. Nat. Clim. Chang. 6: 390–393. https://doi.org/10.1038/nclimate2899.

Miège, C., Forster, R.R., Box, J.E., Burgess, E.W., Mcconnell, J.R., Pasteris, D.R., Spikes, V.B., 2013. Southeast Greenland high accumulation rates derived from firn cores and ground-penetrating radar. Ann. Glaciol. 54 (63):322–332. https://doi.org/10.3189/2013AoG63A358.

Miège, C., Forster, R., Brucker, L., Koenig, L., Solomon, D.K., Paden, J., Box, J., Burgess, E., Miller, J., McNerney, L., Brautigam, N., Fausto, R., Gogineni, S.P., 2016. Spatial extent and temporal variability of Greenland firn aquifers detected by ground and airborne radars. J. Geophys. Res. Earth Surf. 121:2381–2398. https://doi.org/10.1002/2016JF003869.

Miller, O.L., Solomon, D.K., Miège, C., Koenig, L., Forster, R.R., Montgomery, L.N., Schmerr, N., Ligtenberg, S., Legtchenko, A., Brucker, L., 2017. Hydraulic conductivity of a firn aquifer in southeast Greenland. Front. Earth Sci. 5, 38. https://doi.org/10.3389/feart.2017.00038.

Mohnke, O., Yaramanci, U., 2002. Smooth and block inversion of surface NMR amplitudes and decay times using simulated annealing. J. Appl. Geophys. 50:163–177. https://doi.org/10.1016/S0926-9851(02) 00137-4.

Montgomery, L.N., Schmerr, N., Burdick, S., Forster, R.R., Koenig, L., Legchenko, A., Ligtenberg, S., Miège, C., Miller, O.L., Solomon, D.K., 2017. Investigation of firn aquifer structure in southeastern Greenland using active source seismology. Front. Earth Sci. 5, 10. https://doi.org/10.3389/feart.2017.00010.

Mueller-Petke, M., Yaramanci, U., 2010. QT-inversion-comprehensive use of the complete surface-NMR data set. Geophysics 75:WA199–WA209. https://doi.org/10.1190/1.3471523.

Müller-Petke, M., Yaramanci, U., 2008. Resolution studies for Magnetic Resonance Sounding (MRS) using the singular value decomposition. J. Appl. Geophys. 66: 165–175. https://doi.org/10.1016/j.jappgeo.2007.11.004.

Müller-Petke, M., Dlugosch, R., Yaramanci, U., 2011a. Evaluation of surface nuclear magnetic resonance-estimated subsurface water content. New J. Phys. 13. https://doi.org/10.1088/1367-2630/13/9/095002.

Müller-Petke, M., Hiller, T., Herrmann, R., Yaramanci, U., 2011b. Reliability and limitations of surface NMR assessed by comparison to borehole NMR. Near Surf. Geophys. 9: 123–134. https://doi.org/10.3997/1873-0604.2010066.

Pan, J., Li, Z., Zhang, Y., Bernard, J., Chen, L., Gao, L., Xie, M., 2017. Correlating intensity of pulse moment with exploration depth in surface NMR. J. Appl. Geophys. 142:1–13. https://doi.org/10.1016/j.jappgeo.2017.05.005.

Parsekian, A.D., Grombacher, D., 2015. Uncertainty estimates for surface nuclearmagnetic resonance water content and relaxation time profiles from bootstrap statistics. J. Appl. Geophys. 119:61–70. https://doi.org/10.1016/j.jappgeo.2015.05.005.

Poinar, K., Joughin, I., Lilien, D., Brucker, L., Kehrl, L., Nowicki, S., 2017. Drainage of southeast Greenland firn aquifer water through crevasses to the bed. Front. Earth Sci. 5 (5): 2017. https://doi.org/10.3389/feart.2017.00005.

Schirov, M., Legchenko, A., Creer, G., 1991. New direct non-invasive ground water detection technology for Australia. Explor. Geophys. 22, 333–338.

Semenov, A.G., Schirov, M.D., Legchenko, A.V., Burshtein, A.I., Pusep, A.Yu., 1989. Device for measuring the parameter of underground mineral deposit. G.B. Patent 2198540B.

Shushakov, O., 1996. Groundwater NMR in conductive water. Geophysics 61:998–1006. https://doi.org/10.1190/1.1444048.

Slichter, C.P., 1990. Principles of Magnetic Resonance. Springer-Verlag, Berlin Heidelberg.

Tikhonov, A., Arsenin, V., 1977. Solution of Ill-posed Problems. John Wiley & Sons, Inc.

Trushkin, D.V., Shushakov, O.A., Legchenko, A.V., 1995. Surface NMR applied to an electroconductive medium. Geophys. Prospect. 43:623–633. https://doi.org/10.1111/j.1365-2478.1995.tb00271.x.

Valla, P., Legchenko, A., 2002. One-dimensional modelling for proton magnetic resonance sounding measurements over an electrically conductive medium. J. Appl. Geophys. 50:217–229. https://doi.org/10.1016/S0926-9851(02)00141-6.

Vincent, C., Descloitres, M., Garambois, S., Legchenko, A., Guyard, H., Lefebvre, E., Gilbert, A., 2012. Detection of a subglacial lake in Glacier de Tete Rousse (Mont Blanc area, France). J. Glaciol. 58 (211):866–878. https://doi.org/10.3189/2012JoG11J179.

Vouillamoz, J.M., Legchenko, A., Nandagiri, L., 2011. Characterizing aquifers when using magnetic resonance sounding in a heterogeneous geomagnetic field. Near Surf. Geophys. 9:135–144. https://doi.org/10.3997/1873-0604.2010053.

Weichman, P.B., Lavely, E.M., Ritzwoller, M.H., 2000. Theory of surface nuclear magnetic resonance with applications to geophysical imaging problems. Phys. Rev. E Stat. Phys. Plasmas Fluids Relat. Interdiscip. Top. 62 (1):1290–1312. https://doi.org/10.1103/PhysRevE.62.1290.